An evaluation of Ti-in-Quartz Geothermometry using thermally well-constrained quartzites from the aureole of the Ballachulish Igneous Complex, W. Scotland.

Mike Jollands, School of Earth and Environment, University of Leeds, LS6 9JT

Titanium-in-Quartz geothermometry, originally pioneered by *Wark and Watson* [2006] then later modified by *Kawasaki and Osanai* [2008] and *Thomas et al.* [2010] promises accurate quartz crystallisation temperature determinations from straightforward measurements of Ti within the quartz lattice. These geothermometers are tested by applying them to a suite of contact metamorphosed quartzites from around the Ballachulish Igneous Complex in West Scotland. Results show that the original Ti-in-Quartz geothermometer gives results broadly in agreement with thermal modelling and pre-existing geothermometry data from Ballachulish and the latter geothermometers give temperatures which are consistently too low. However, despite a broad agreement between published temperature values and those derived from the original thermometer of *Wark and Watson* [2006], there is a lack of correlation between distance from the igneous contact and determined temperature, as well as unacceptably large errors in some cases.

Furthermore, a rigorous test of the methodology employed in this and other studies suggests that the system is more complex than assumed, and a greater understanding of the substitution of other elements in quartz (such as aluminium) is necessary.

In addition, various issues have been raised by other workers regarding the validity of Ti-in-Quartz as a geothermometry tool at all, inasmuch as the original equations were constructed with a disregard for a range of complicating factors. This study adds further weight to a growing mass of critiques of this technique of geothermometry and suggests a much greater understanding of the processes is necessary before Ti-in-Quartz can be convincingly upheld as a viable tool.

1) Introduction

Quartz, whilst common in crustal rocks, is generally of limited use in temperature determinations. Work has previously focussed on aluminium in quartz [*Dennen et al.*, 1970; *Götze et al.*, 2001], 'fractal' geometry [*Kruhl and Nega*, 1996; *Mamtani and Greiling*, 2010; *Wu et al.*, 2006], thermoluminescence [*Sawakuchi et al.*, 2011], c-axis opening angles [e.g. *Thigpen et al.*, 2010] and importantly for this study, titanium in quartz [*Wark and Watson*, 2006] to give quartz crystallisation temperatures, with variable success.

The Titanium-in-Quartz (TitaniQ) geothermometer of *Wark and Watson*, [2006] (Equation 1), is based on empirical measurements of Ti incorporated into synthetic quartz formed between 600-1000°C at 1GPa, where a_{Ti}=1(i.e. rutile is present). Temperature (T) is given in degrees centigrade from input of the X_{Ti}^{Qtz} coefficient, which represents Ti (ppm) within the quartz lattice.

$$T(^{\circ}C) = \frac{-3765}{\log\left(X_{Ti}^{Qtz}\right) - 5.69} - 273$$

Equation 1

It is based on the known temperature-dependent diffusivity (D_{Ti}) of Ti in quartz (Equation 2 [where R is the gas constant at 8.314JK^{-1}]), where Ti^{4+} moves by lattice diffusion, substituting for Si^{4+} within the quartz framework [*Cherniak et al.*, 2007]. Due to Ti^{4+} existing in 6-fold coordination with O^{2-} compared to Si^{4+} in 4-fold coordination with O^{2-}, this is a high temperature substitution, and may become unstable on cooling [*Blankenburg et al.*, 1994] in *Götze et al.* [2004].

$$D_{Ti} = 7 \times 10^{-8} \exp\left(\frac{-273 \pm 12 kJmol^{-1}}{RT}\right) m^2 \sec^{-1}$$

Equation 2

Originally devised and used for temperature determinations in hydrothermal quartz [*Müller et al.*, 2010; *Rusk et al.*, 2008, *Wark and Watson*, 2006], the TitaniQ technique was later used in granulites [*Sato and Santosh*, 2007], rhyolites [*Vazquez et al.*, 2009; *Wark et al.*, 2007], migmatites [*Spear and Wark*, 2009; *Storm and Spear*, 2009], mylonites [*Adamson*, 2010; *Kohn and Northrup*, 2009], porphyry quartz veins [*Müller et al.*, 2010] and granites [*Wiebe et al.*, 2007]. The original TitaniQ geothermometer was later refined to include a pressure coefficient by *Thomas et al.* [2010], supposedly

allowing temperature determinations from known pressure, and vice versa (Equation 3).

$$T(^{\circ}C) = \frac{(60952 \pm 3122) + (1741 \pm 63)P(kbar)}{(1.520 \pm 0.04) - R\ln X_{TiO_2}^{Qtz} + R\ln a_{TiO_2}} - 273$$

Equation 3

A granulite-derived Ti-in-Quartz geothermometer was later developed by *Kawasaki and Osanai*, [2008] using natural rocks from Antarctica (Equation 4). This, and the geothermometer of *Thomas et al.* [2010] both use $X_{TiO_2}^{Qtz}$ (mole fraction Ti) instead of X_{Ti}^{Qtz} (ppm Ti).

$$T(^{\circ}C) = \frac{-5895}{\ln X_{TiO_2}^{Qtz} + 1.729} - 273$$

Equation 4

Recently, *Wilson et al.*, [in press] has cast doubt on the validity of any Ti-in-Quartz geothermometry due to the poorly constrained speciation of Ti in any fluids involved. This study, following on from the work of *Adamson* [2010] at the University of Leeds aims to add further evaluation to the TitaniQ geothermometer using a suite of thermally well-constrained contact-metamorphosed rocks from the Ballachulish Igneous Complex in North Scotland.

1.1) Geological Setting

The Ballachulish Igneous Complex (BIC) is located at Ballachulish, near Fort William in Argyllshire, West Scotland (Figure 1.1). It sits within the Grampian Highland geological province, near to the Great Glen Fault, which forms its northernmost limit [*Voll*, 1991].

Figure 1.1: Location of Ballachulish, near Fort William on the west coast of Scotland.

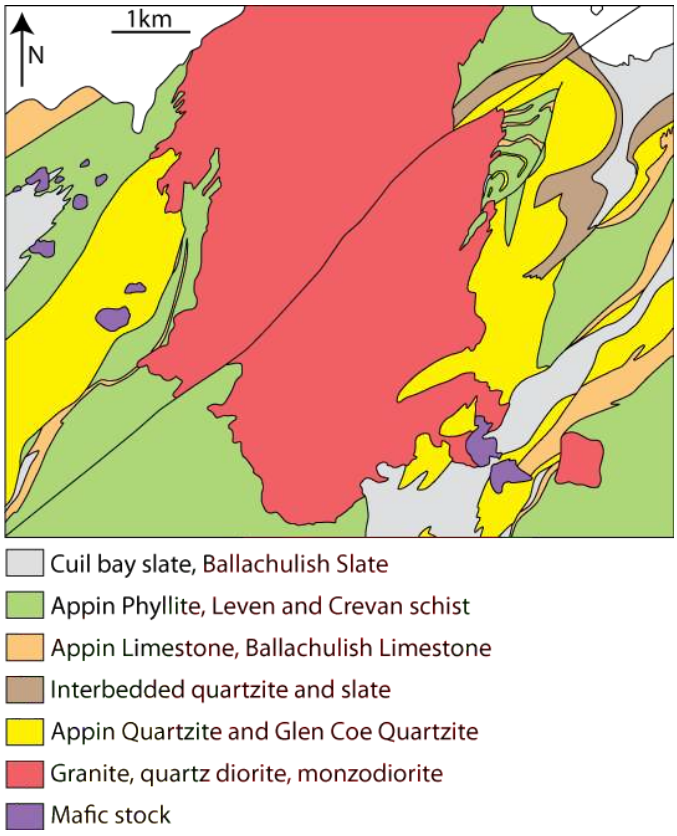

Figure 1.2: Simplified geological map of the BIC.

The BIC is comprised of granite, monzodiorite and quartz diorite intruded as an approximately cylindrical body, with granite in the centre and quartz diorite at the perimeter [*Buntebarth*, 1991]. The intrusion is related to the waning stage of the Ordovician-Devonian Caledonian Orogeny [*Voll*, 1991], with igneous activity post-dating regional metamorphism [*Bailey and Maufe*, 1960]. Early attempts at dating the BIC gave 412±28M.a. [*Weiss and Troll*, 1991], later confirmed by $^{207}Pb/^{206}Pb$ and $^{206}Pb/^{238}U$ dating giving 427±1M.a. and 423±0.3M.a. respectively [*Fraser et al.*, 2004].

A variety of metasediments from the Dalradian supergroup are intruded into [*Voll*, 1991], including, most importantly for this study, the Appin quartzite (Figure 1.2). The Appin quartzite, part of the Ballachulish subgroup of the Lower Dalradian Appin Group [*Pattison and Voll*, 1991] is composed of around 85% quartz, with the remaining 15% being feldspars (predominantly alkaline) [*Buntebarth and Voll*, 1991], and accessory apatite, tourmaline, zircon, titanomagnetite, monazite and rutile. The rock has a bimodal grain size distribution [*Hoernes and Voll*, 1991], with common cross bedding and graded bedding [*Pattison and Voll*, 1991]. The palaeo-environment is

suggested to be a NE-prograding tidal delta formed in a tectonically stable environment [*Lind*, 1996; *Voll*, 1991].

1.2) Thermal Conditions in the Aureole

Thermal modelling of the aureole [*Buntebarth*, 1991] along with geothermometry data [*Kroll et al.*, 1991; *Masch and Heuss-Assbichler*, 1991; *Pattison*, 1991] show an exponential decrease in temperature away from the igneous contact (Figure 1.3). A depth of intrusion of around 10km [*Pattison*, 1989] suggests the country rocks were 250-300°C pre-emplacement, assuming a normal geothermal gradient. Maximum temperatures of 1100°C were attained within the igneous body [*Weiss and Troll*, 1989], leading to contact-metamorphism of the country rock at up to 850°C [*Lind*, 1996], although estimates vary. Contact metamorphism is thought to have lasted around 500k.y., including around 270k.y. during which conditions were hot enough to cause partial melting [*Pattison and Harte*, 1997].

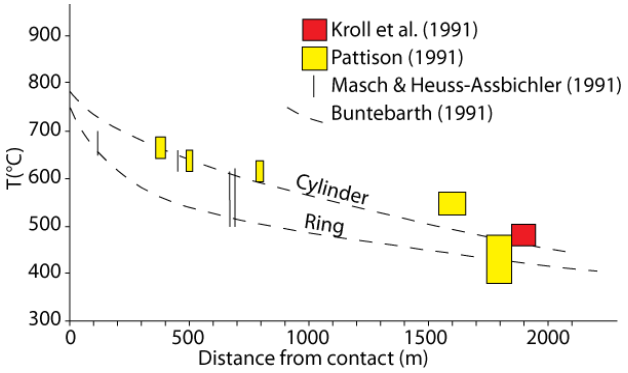

Figure 1.3: Thermal profile in the contact aureole of the BIC, constrained by modelling and geothermometry.

Using a suite of Appin Quartzite rocks, with known geographical distribution, collected by *Lind*, [1996], this study aims to test the validity of Ti-in-Quartz as a geothermometer. The temperature of the aureole is considered as a known value to a reasonable degree of accuracy (Figure 1.3), as is distance from the igneous contact for each sample. Hence by determining the concentration of Ti in quartz and with it crystallisation temperatures for a variety of samples, the validity of the geothermometer equations can be assessed.

2) Methodology

Polished, carbon coated blocks of quartzite samples taken from known distances from the surface exposure of the igneous intrusion were imaged using backscattered electron (BSE) imaging on an FEI Quanta 650 scanning electron microscope (SEM). Major and minor phases present were identified using an attached Oxford Xmax 80 energy-dispersive X-X-ray spectrometer (EDS). Areas consisting of quartz with rutile were identified in BSE and then imaged by cathodoluminescence (CL) using a KE Centaurus panchromatic CL detector.

Subsequently, the rims of quartz grains from 4 samples showing high luminescence were analysed using Laser Ablation-Inductively Coupled Plasma-Mass Spectrometry (LA-ICP-MS) comprising a Geolas Q laser connected to an Argilent 7500c ICP-MS. Spot sizes of 100µm and 15J beam energy were necessary to derive a measurable quantity of titanium whilst maintaining a acceptable resolution. A laser pulse repetition rate of 5Hz for 200 counts was used following around 20-30 seconds of background measurement. Data were then processed using the SILLS software package of *Guillong et al.* [2007] against an NIST SRM610 glass standard [*Pearce et al.*, 1997]. Along with Ti and Si, Na, K, Ca and Al concentrations were determined in order to ensure than the grains ablated were indeed quartz, and not feldspar.

Four quartzite samples were then analysed using a Jeol JXA-8230 electron microprobe. Analytical parameters were set according to the 'optimum' of *Storm and Spear* [2009]. The beam was circular with a diameter of 5µm, 20kV accelerating voltage and 50nA beam current. Counting time was set as 200s on peak, and 100s at each background position above and below the peak. Ti concentration was determined simultaneously using three wavelength dispersive spectrometers (two employed high intensity PET crystals and one a high intensity LIF crystal) and averaged using the Jeol ZAF software package, giving concentrations in increments of 10ppm Ti (10^{-3}wt%). A fixed concentration of 100% silica was assumed.

3) Results

3.1) Scanning Electron Microscopy

Six samples were imaged using SEM. These were selected due to their distance from the igneous contact (Table 1) and relative purity of quartzite.

Sample Number	Distance from Contact / m
56148	2
56165	215
56158	260
56183	325
56169	650
56167	900

Table 1: Samples imaged using SEM, with distance from surface exposure of the igneous contact.

a: 56148

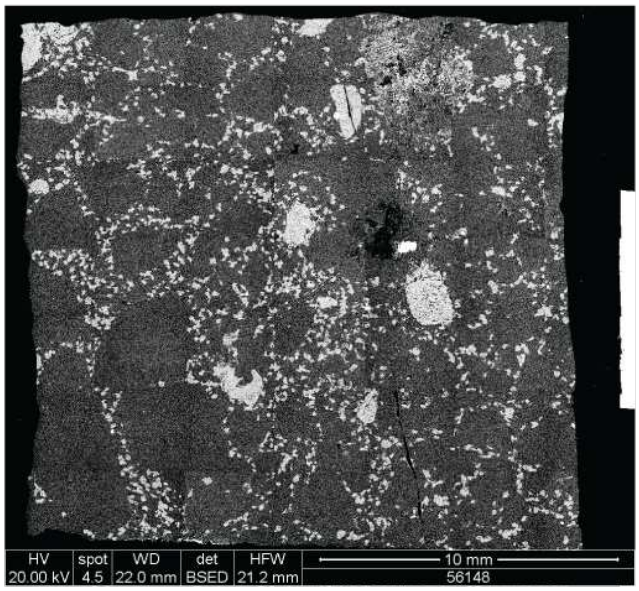

d: 56183

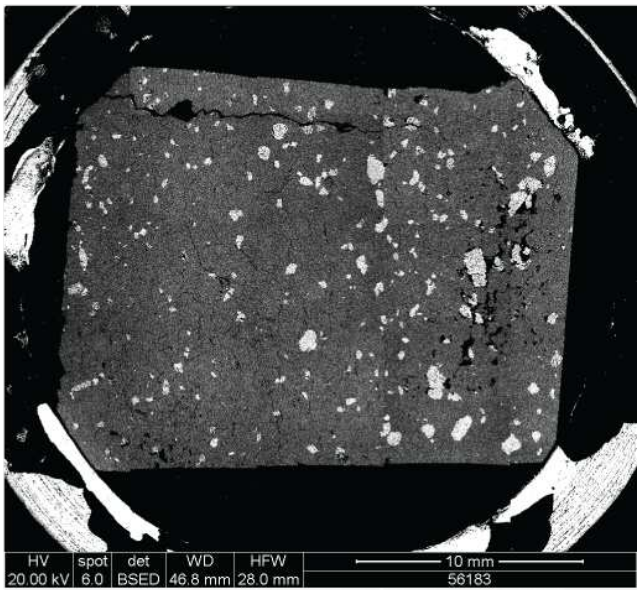

b: 56165

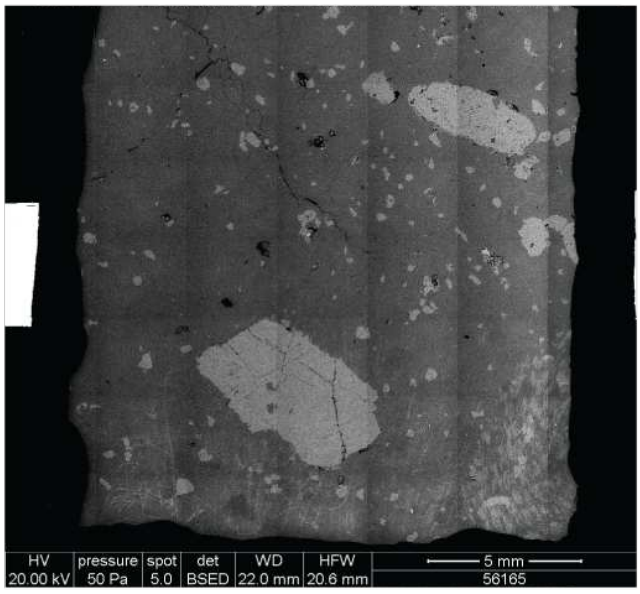

e: 56169

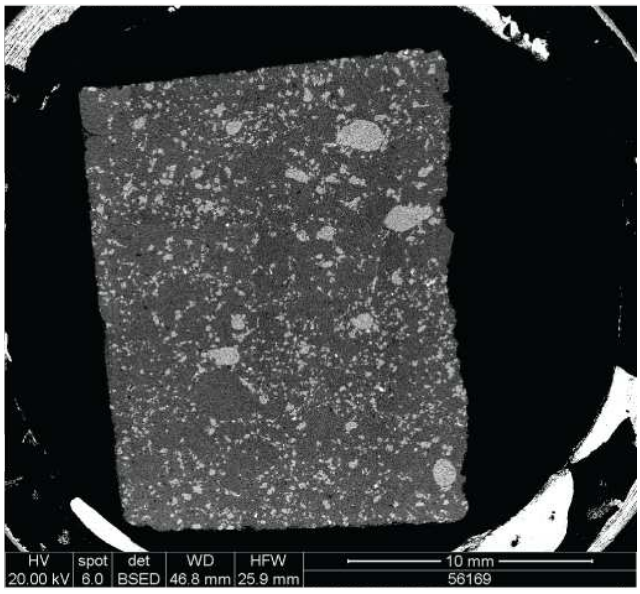

c: 56158

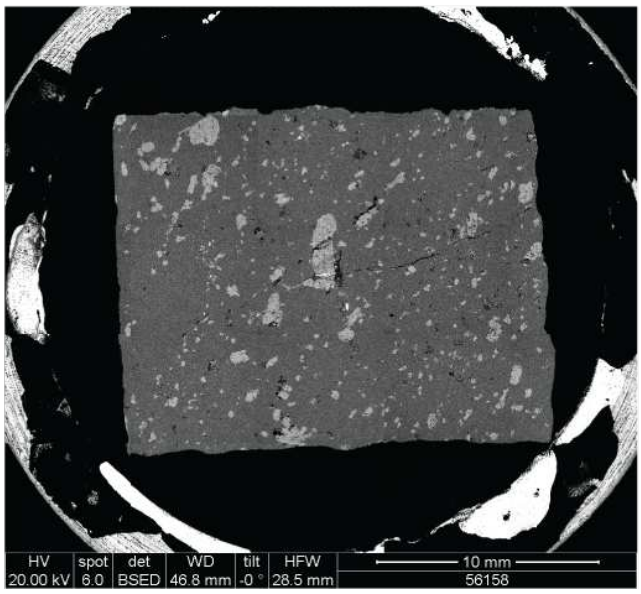

f: 56167

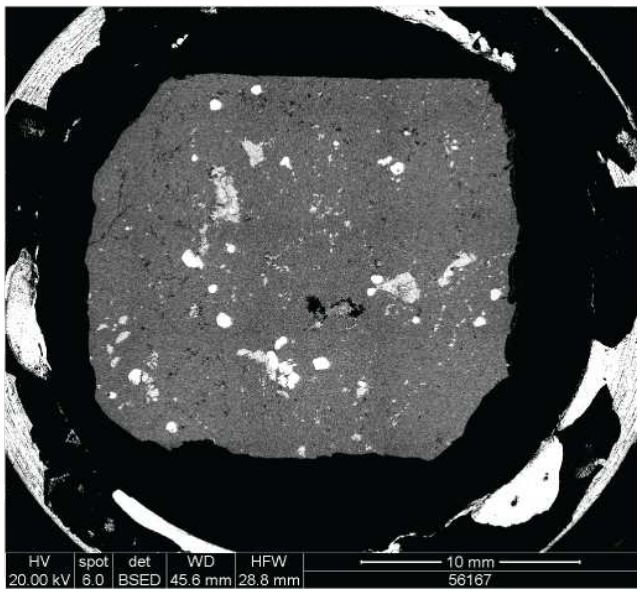

Figure 3.1: BSE contrast montages of all six samples selected for analysis. The predominant mid-grey phase is quartz, with the secondary paler grey phase being feldspar (generally alkali). Bright white phases are a variety of accessories, described in text.

BSE montages of the six samples are shown in Figure 3.1. In all cases, the dominant mid-grey phase in quartz, with the abundant paler grey phase being feldspar (dominantly alkali-feldspar with minor plagioclase). Black areas generally represent surface imperfections, and bright white areas are a variety of accessory phases, including apatite, titanite, muscovite, rutile, zircon, monazite, titanomagnetite and Fe-oxides. For the purpose of this study the positive identification of rutile (TiO_2) is important as it suggests the activity of Ti (a_{Ti}) is 1 (if rutile is assumed to be pure TiO_2). This simplifies the use of the Ti-in-Quartz geothermometer, as corrections for activity need not be made [*Wark and Watson*, 2006].

3.2) Cathodoluminescence

Quartz-rich areas within the six samples were then imaged using cathodoluminescence, which revealed a variety of complex textures within the quartz grains. These were described in detail at Ballachulish by *Lind* [1996] and later refined by *Holness and Watt* [2001]. The latter defined five types of quartz visible by CL:

Type 1: Dark and mottled quartz, with irregular bright patches, found in the cores of grains (Figure 3.2a,b). Suggested to be relict from regional metamorphism [*Holness and Watt*, 2001].

Type 2: Alternating bright and dark bands, generally

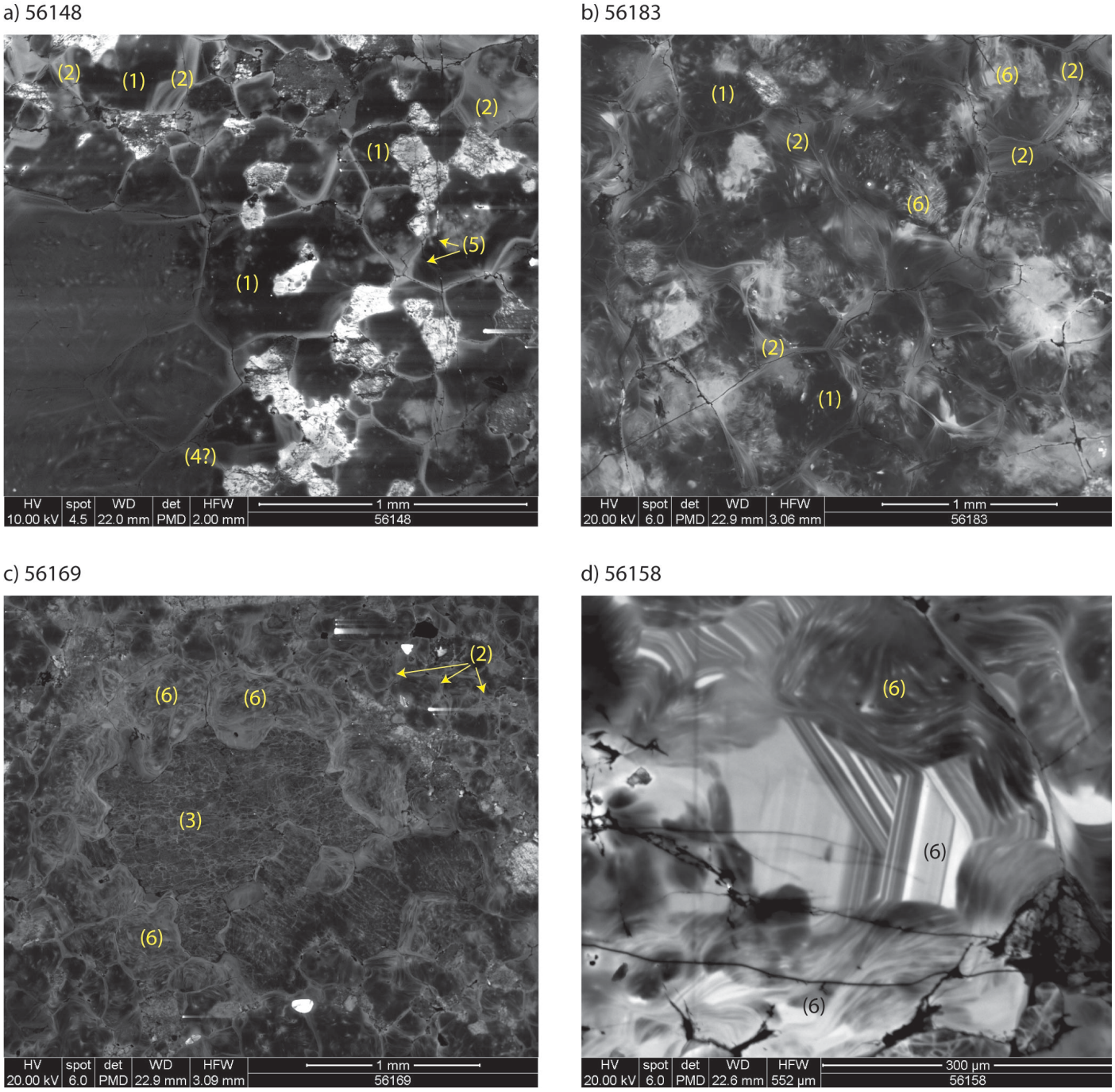

Figure 3.2: CL images of various samples to illustrate the different 'types' of quartz present. Numbers refer to description in text.

parallel or subparallel to grain margins (Figure 3.2a,b,c). These are thought to relate to grain-boundary migration during growth at the onset of contact metamorphism [*Lind*, 1996].
Type 3: Bright linear features within grains, generally with no relation to grain margin orientation (Figure 3.2c). Suggested to result from cracking and sealing close to intrusion [*Holness and Watt*, 2001].
Type 4: Brightly luminescing quartz on grain boundaries, with no fine scale banding (Figure 3.2a). May relate to melt migration along grain boundaries and cracks [*Holness and Watt*, 2001].
Type 5: Non-luminescent linear features, crosscutting all earlier grains (Figure 3.2a). These relate to fracture healing from late fluid migration [*Holness and Watt*, 2001]

Along with the five types recognised above, one additional type will be added to classify all quartz types seen:

Type 6: Luminescent quartz with alternating light and dark bands. In some cases this has straight bands with clear truncation relationships (Type 6a; Figure 3.2d[centre]), suggesting an igneous origin (D. Morgan, *pers. comm.*), and in others has wavy bands with poor definition (Type 6b; Figure 3,2b,c,d). It is suggested that the light to dark alteration is preserved igneous banding from primary quartz grain growth (comparable to the oscillatory zoning in feldspars described by *Allègre et al.*, [1981]), and that where the banding is wavy it has been metamorphosed. In most cases the banding is only wavy, but in one spectacular example the banding shows straight zoning grading into wavy suggesting a clear genetic link.

The bright edges of quartz grains seen in Figure 3.2, generally the Type 2 quartz of *Holness and Watt*, [2001] is assumed to have experienced the effects of contact metamorphism from intrusion of the Ballachulish Igneous Complex. Therefore, if the concentration of Ti in quartz is indicative of the temperature reached during this event, it should be recorded only in quartz present at the edges of grains. This is in agreement with the conclusions of *Adamson* [2010].

3.3) LA-ICP-MS

Laser-ablation analysis was performed on four samples, 56183, 56167, 56158 and 56148. Poor imaging connected to the laser meant that it was not always clear if the laser was ablating pure quartz or feldspar. Furthermore, the spatial resolution (100μm spot) and depth of sampling into the specimen readily allowed contamination by accessory mineral phases, including rutile. The simultaneous measurement of Na, Al, Si, K, Ca and Ti allowed ablations aimed inadvertently at feldspars (highly elevated Na, Ca, K depending on feldspar type)

Sample	Ti / ppm	Geothermometer Temperatures		
		Wark & Watson (2006)	Thomas et al. (2010)	Kawasaki & Osanai (2008)
56148	166	812	646	418
56148	114	764	607	388
56148	133	783	623	400
56148	20	586	466	279
56148	27	612	487	295
56158	25	604	481	291
56158	24	602	479	290
56158	38	644	512	315
56158	18	576	458	273
56158	31	623	496	302
56183	40	649	517	318
56183	35	634	504	309
56183	46	662	527	326
56183	61	691	550	344
56183	36	638	508	311
56167	37	642	511	314

Table 2: Ti in quartz as determined by laser ablation, along with temperatures calculated from the three geothermometers. Significantly more analyses than this were originally taken, but subsequently were discarded due to contamination by feldspar or rutile, or where Ti detection in the mass spectrometer was within error of the background measurement.

and rutile needles (anomalously high Ti) to be discarded, following the recommendation of *Adamson* [2010]. Samples showing Ti concentrations within three standard deviations of the detection limits were also removed. The remaining analyses, with calculated temperatures given by the three aforementioned geothermometers are given in Table 2.

Temperatures calculated by the geothermometers of Thomas et al (2010) and Kawasaki & Osanai (2008) are anomalously low relative to those predicted by thermal modelling [*Buntebarth*, 1991], whereas the temperatures from the *Wark & Watson* [2006] 'TitaniQ' geothermometer straddles the modelled values. There is, however, no clear distance-temperature correlation, especially if the closest sample is omitted.

3.4) EPMA (Electron-Probe Micro-Analysis)

Microprobe analysis was performed on four samples; 56169, 56183, 46148 and 56158. Sixty measurements of Ti content (ppm) were taken from each sample, in a combination of spot analyses and line analyses (comprising a series of spots with fixed spacing). All spots were located in the brightly luminescing grain boundaries ('Type 2 quartz'), and lines were generally perpendicular to banding ('Type 2' or 'Type 6'), usually also including non-luminescent grain centres ('Type 1').

Average Ti concentrations (ppm) along with calculated crystallisation temperatures for each sample are given in Table 3 and shown in figure 3.4, with the full data set available in Appendix 1. Again, the TitaniQ values lie around the modelled temperatures, but there is no clear distance-temperature relationship. If the closest sample is omitted, the 3 further samples show an increase in temperature away from the contact.

Concentrations of Ti determined from line analyses, along with relevant greyscale along the lines from associated CL images are given in Figure 3.5. These are taken from a variety of quartz types in different settings, and will be more comprehensively discussed below.

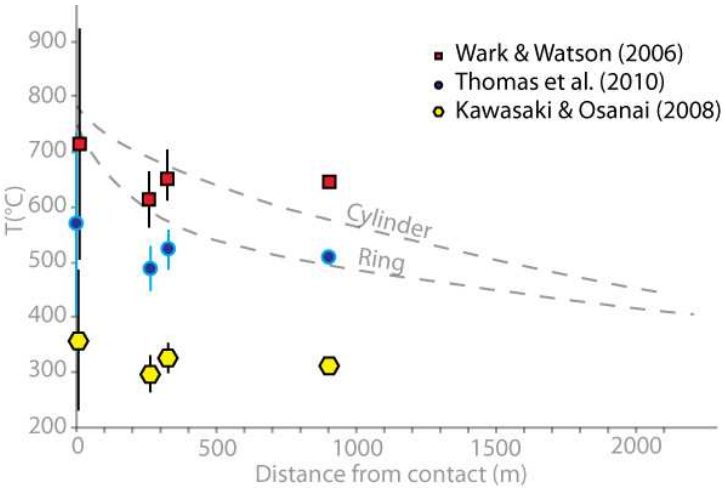

Figure 3.3: Temperatures determined from LA-ICP-MS analysis with three geothermometers. Error bars are two standard deviations above and below the mean, representing 95% confidence limits. Note extremely large spread closest to the contact representing highly variable Ti contents. The lack of error bars at the furthest point is due to only one Ti measurement being considered valid, hence standard deviation cannot be calculated.

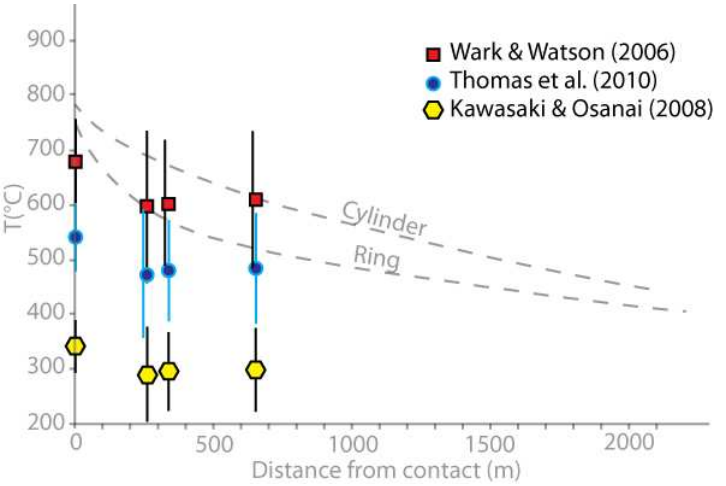

Figure 3.4: Temperatures determined from EPMA analysis by three geothermometers, with error bars as in Figure 3.3. Error in all samples is relatively constant with around ±100°C spread around the mean falling within 95% confidence limits.

Sample	Ti / ppm	Geothermometer Temperatures		
		Wark & Watson (2006)	Thomas et al. (2010)	Kawasaki & Osanai (2008)
56148	53	676 (39)	538 (31)	341 (24)
56158	22	593 (69)	472 (56)	290 (43)
56183	24	601 (57)	478 (45)	295 (35)
56169	26	607 (62)	483 (50)	299 (38)

Table 3: Average Ti concentration in each sample as determined by EPMA, along with calculated temperatures from each geothermometer. Values in brackets represent one standard deviation.

a) 56148_031

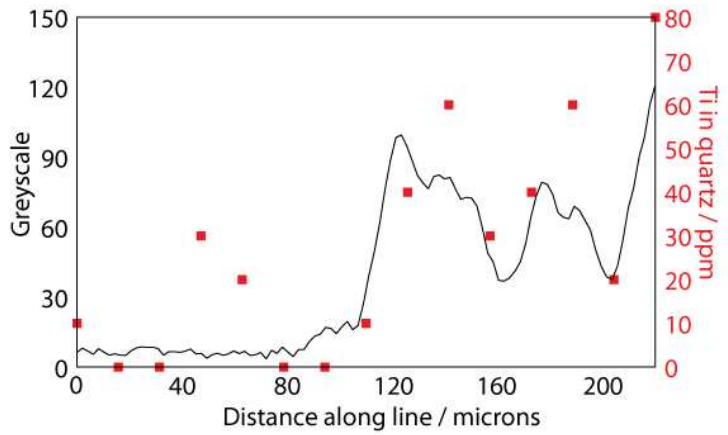

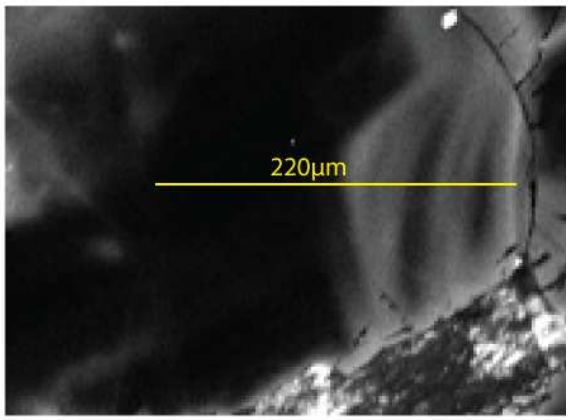

b) 56148_054

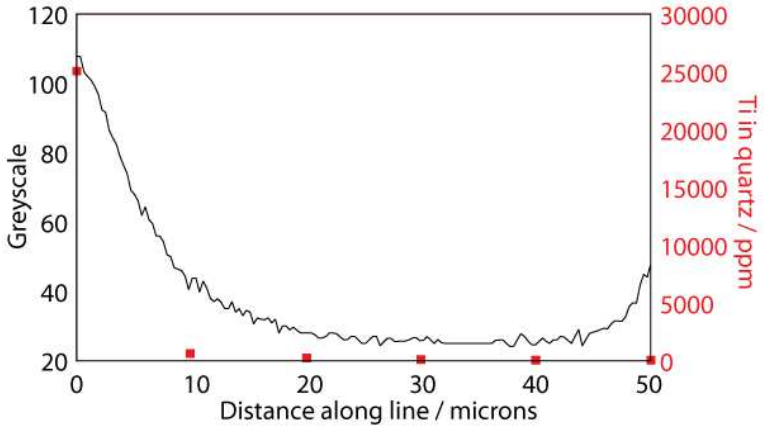

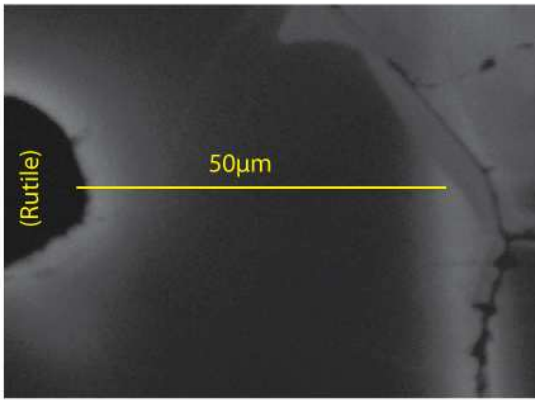

c) 56158_004

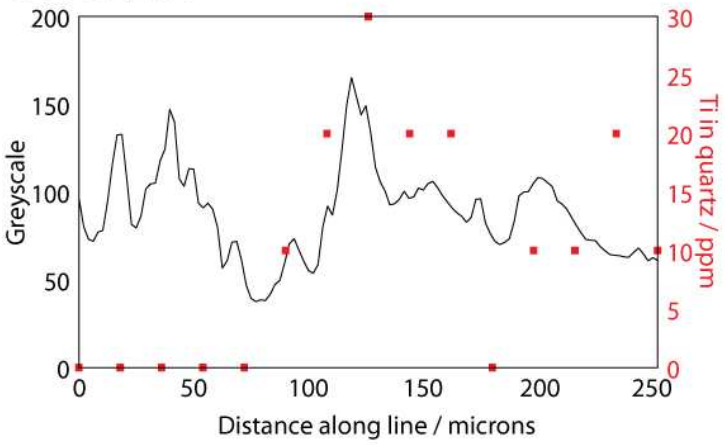

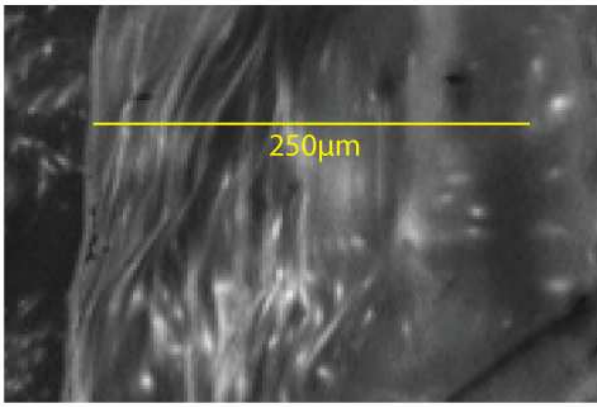

d) 56158_028

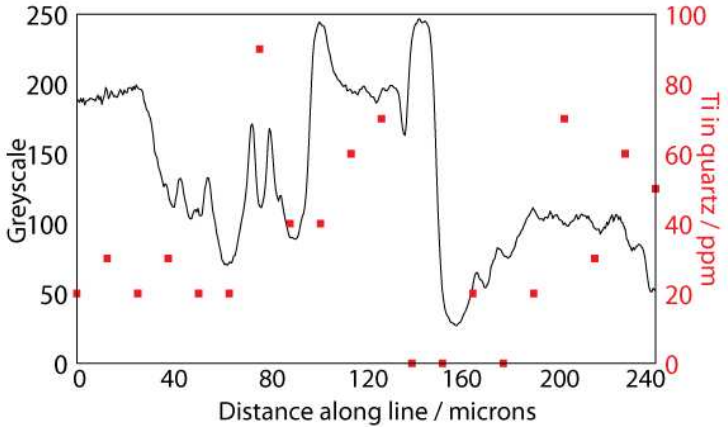

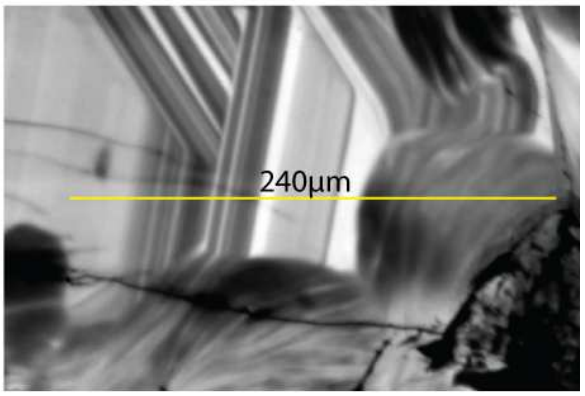

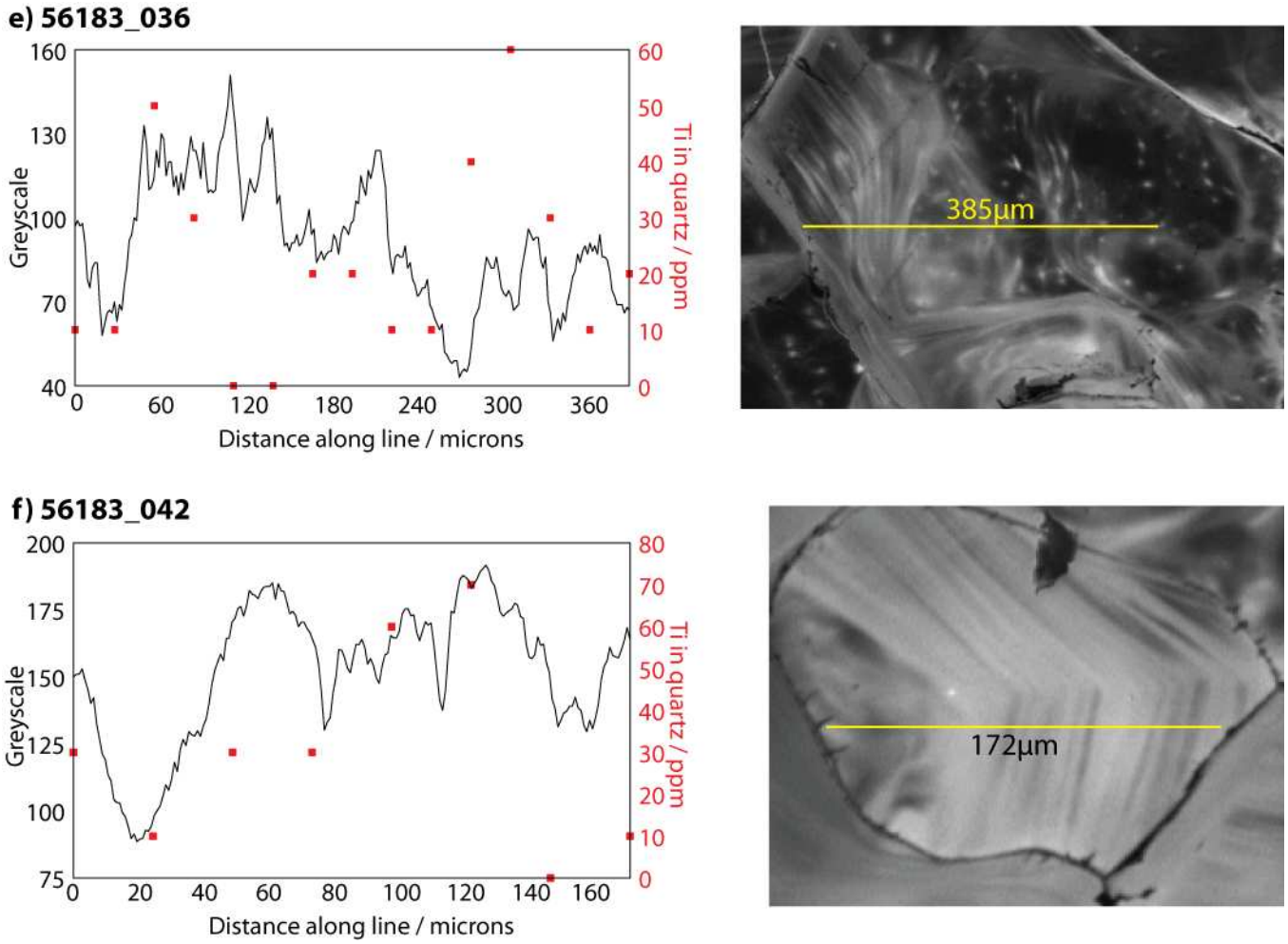

Figure 3.5: Locations of line analyses on CL images (yellow line), along with the greyscale profile (solid black line) and point analyses of Ti in quartz (red squares). Note the highly elevated Ti concentration in (b) due to sampling directly from the edge of a rutile grain.

4) Discussion

4.1) Issues with the methodology

As mentioned above, this study is a continuation of previous work conducted by *Adamson* [2010] at the University of Leeds on Moine Thrust mylonite temperatures. The methodology used in this report was an adapted version of that suggested in his study. Issues were identified with all stages in the method with the exception of straightforward BSE imaging. These are discussed below.

Use of LA-ICP-MS

Following mapping of brightly-luminescing regions at quartz grain boundaries, attempts were made to locate these areas and subject them to laser-ablation. However, the very different styles of imaging in the SEM-CL detector (electron microscope) and the laser ablator (equipped with a low powered optical microscope without petrological capabilities) made correlation between the two machines nearly impossible. Attempts were made to produce a series of accurate grid references for alignment, but this was unsuccessful, probably due to sample rotation when mounting below the laser (any mismatch in sample orientation between the SEM and LA-ICP-MS would lead to large variations in location when using simple (x,y) co-ordinates). Hence, all analyses were taken at any visible grain boundaries. This allowed the possibility of accidental ablation of feldspar (quartz and feldspar were almost indistinguishable), and also meant there was no control on which 'type' [*Holness and Watt*, 2001] of quartz had been ablated.

Furthermore, the sampling resolution of 100µm is generally much greater than the scale of visible zoning in

quartz [*Müller et al.*, 2003], hence the laser will essentially take an average value of Ti concentration in the entire sampled area, which is deep as well as wide (Figure 4.1).

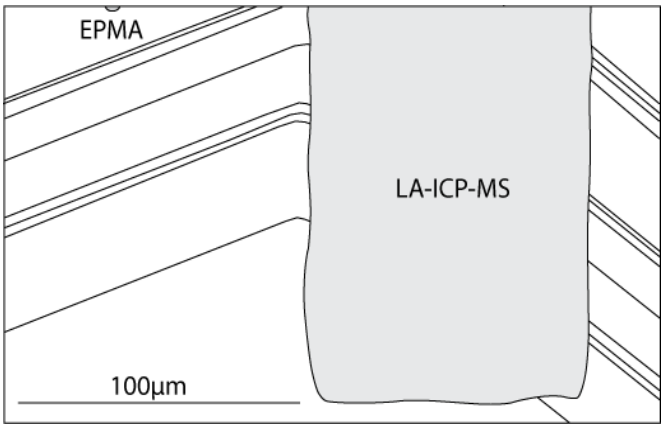

Figure 4.1: The difference in sample size taken by LA-ICP-MS and EPMA, relative to representative zoning in a quartz crystal. After *Müller et al.* [2003].

Use of EPMA

Correlating the CL images between SEM-CL detector and microprobe was simple due to the use of the same imaging system in both machines. The LA-ICP-MS problem of poor sampling resolution was also resolved when using the microprobe by a selection of 5µm spot size.

However, this technique gave lower precision compared to laser ablation; where laser ablation gave precision to a ppm level, the microprobe was only able to give values to the nearest 10ppm. This is generally not problematic unless the concentration of Ti is between 0 and 5ppm, and is subsequently rounded to 0ppm. Because all geothermometers used include an exponential function, a concentration of 0ppm Ti invalidates the formulae.

Furthermore, calibration of the probe was not possible due to a lack of Ti-in-Quartz standard, so the accuracy of this method is essentially unknown. The values calculated by the microprobe software may be consistently misplaced from the actual titanium concentration, which could help explain the different values given by EPMA and LA-ICP-MS. If work on Ti-in-Quartz geothermometry is to continue, it is of critical importance that a standard is produced for calibration.

Use of CL prior to EMPA/LA-ICP-MS

Cathodoluminescence, whereby a beam of electrons from an SEM causes a luminescent material (such as quartz) to emit visible light [*Reed*, 1996] was used to determine the 'best' areas of quartz grains for further analysis. This was based on an assumption inherited from *Adamson* [2010] and others [e.g. *Rusk et al.*, 2006; *Spear and Wark*, 2009] that the brightest areas in CL would have been most affected by metamorphism, and hence would have the greatest Ti concentration, giving peak temperature of quartz crystallisation.

This assumption has been tested using the line analyses shown in Figure 3.5. Continuous measurement of the CL greyscale (0-255) against discontinuous measurements of Ti concentration (from line analyses) are shown. If the most brightly-luminescing areas have the highest Ti concentration, then positive correlation between greyscale and Ti (ppm) should be expected at each spot. However, the degree of correlation varies from no correlation (Figure 4.2d,e) through weak (Figure 4.2c,f) to strong positive (Figure 4.2a,b).

Therefore, where rutile is present there is a clear link between CL intensity and Ti content in quartz, but in other cases there is no correlation at all. It may be that another trace contaminant of quartz, possibly aluminium and lithium [*Perny et al.*, 1992] are activating the CL zoning, or alternatively are responsible for creating crystal defects which in turn cause luminescence [*Watt*, 1997]. Other candidates for CL activation are K^+, Na^+ and Fe [*Landtwing*, 2005]. It has also been suggested that Ti only becomes the primary CL activator in very high temperature quartz [*Rusk et al.*, 2008], and at lower temperatures (possibly including those observed at Ballachulish) it may be a secondary or lower CL activator.

Therefore, the initial assumption that the rims of quartz crystals represent the maximum crystallisation temperatures with respect to Ti concentration in quartz is not valid for all cases, except where rutile is clearly present.

4.2) Issues regarding the use of Ti-in-Quartz Geothermometry

The original stated aim of this study was to determine the validity of Ti-in-Quartz geothermometry by testing it on thermally well-constrained rocks from Ballachulish. The previous section concerned issues with the methodology used to gain Ti values from the samples, but there are also potential pitfalls with the geothermometer itself. These are discussed below.

Use of the X_{Ti}^{Qtz} parameter

The original TitaniQ geothermometer [*Wark and Watson*, 2006] used X_{Ti}^{Qtz}, the concentration of Ti in ppm, to determine temperature. This has been criticised by *Kawasaki and Osanai* [2008] who suggest that the mole fraction coefficient is much more appropriate when

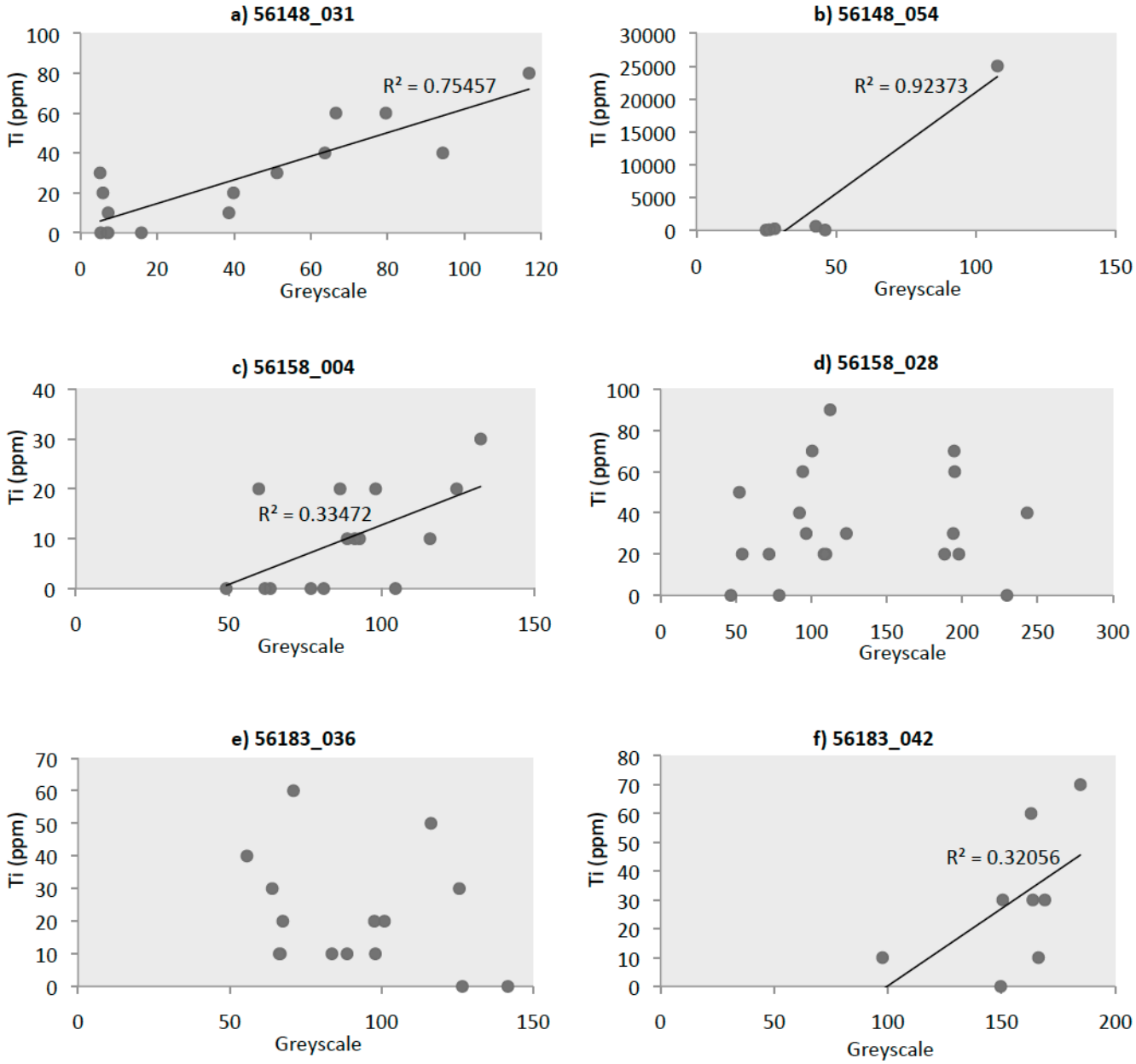

Figure 4.2: Measured concentration of Ti (determined by EPMA) against greyscale from CL images averaged over 5µm for the line analyses shown in Figure 3.5. Trend lines are determined by Microsoft Excel using the least squares method, and relevant R^2 values are given. Figures (d) and (e) show no correlation, and (c) and (f) show very weak correlation. Figures (a) and (b) both have high R^2 values, with the correlation in (a) considered to be the strongest as that in (b) relies on a single point.

deriving the geothermometry equations from thermodynamic first principles. However, this may not be problematic for TitaniQ, as it was originally derived from empirical data and was not a thermodynamic construct.

Assumption that $a_{Ti}=1$ (where rutile is present)

Whilst the TitaniQ geothermometer may be used where rutile is not present (hence $a_{Ti}\neq1$), it is, in its simplest form, based on an assumption that where rutile is present the activity of Ti is 1 [*Wark and Watson*, 2006]. This may not be valid due to kinetic limitations [*Spear and Wark*, 2009] in that Ti from rutile grains may not be able to diffuse around the entire quartz crystal rim before the system is closed to diffusion during cooling.

Furthermore, experimental evidence [*Hayden and Watson*, 2007] suggests that true saturation of rutile within melts will rarely be reached, and is unlikely in

most conditions where Ti-in-Quartz geothermometry is currently employed.

Pressure Effect
The initial TitaniQ geothermometer did not take into account any effects pressure may have on Ti diffusion in quartz. As the Ti-O covalent bond is around 10% longer than the equivalent Si-O bond within quartz tetrahedra [*Thomas et al.*, 2010], higher pressures will favour the more compact Si-O bond, and hence inhibit substitution of Ti for Si and hence Ti diffusion. However, the temperatures determined from the pressure-sensitive geothermobarometer of *Thomas et al.* [2010] are further from the modelled temperatures than those from the original TitaniQ geothermometer (Figures 3.3, 3.4), suggesting this is not an issue for the Ballachulish samples.

Speciation of Ti within the fluid phase
It was suggested above that type 2 and type 4 quartz represented growth from a fluid and melt respectively during contact metamorphism at Ballachulish. Fluid flow at Ballachulish is likely to have been predominantly through fracture networks [*Holness and Clemens*, 1999] with only minor grain boundary flow (due to permeability contrasts). If a fluid is present, it is likely to be the dominant medium of Ti transportation to the extent that any geothermometry will be essentially measuring the degree of speciation between rutile and the aqueous fluid/melt [*Wilson et al.*, in press]. In this scenario, the quartz serves only to record the effects of this process.
The pressure, temperature, pH and Eh of such a fluid will determine which aqueous species of Ti is present, which directly affects solubility of Ti, as well as the degree of partitioning of Ti into a quartz lattice. Furthermore, if any halogens or other ligand-forming chemicals are present, the situation becomes still more complex as a vast range of ionic compounds (some poorly-understood) are formed [*Wilson et al.*, in press].

4.3) Further Complications relating to the Geological Setting

Sample analysis was based on the distance from intrusion data collected by *Lind* [1996]. This took the shortest horizontal distance between the outcrop and the igneous contact, based on surface exposures. It does not account for variations in the three-dimensional geometry of the igneous-wall rock contact, in that with a sloping contact samples will generally be closer to the contact in three dimensions than they are in two dimensions. However, if the assumption of *Buntebarth* [1991] of a cylindrical body with near-vertical walls is correct, this is not an issue.

Buntebarth [1991] also highlights the fact that many variables may impact temperature in an aureole, including magma convection (rate and nature), amount of fluid released, wall-rock permeability, and wall-rock homogeneity.

4.4) Interpretation of Results

Whilst there are clearly problems with the methodology used to derive Ti concentrations from quartz, the formulation of the geothermometer equations and a variety of other complicating factors, the results in Figures 3.3 and 3.4 show that *Wark & Watson's* [2006] TitaniQ geothermometer agrees with previous temperature estimations, within error. However, there is not a clear correlation between TitaniQ-derived temperature and distance from the contact. In EPMA, the closest sample gives the highest temperature but the other three show a slight increase in temperature away from the contact, whereas is LA-ICP-MS the closest sample shows the greatest temperature and the other three show no clear pattern.

Furthermore, the results from this study may agree with previous temperature estimations within error, but the error in some cases is huge (up to ±200°C) making this statistically insignificant.

Whilst the temperature estimations may be reasonable in some cases, the large error, lack of distance-temperature correlation and poor confidence in the methodology leads the author to suggest that any results in good agreement with thermal modelling are not more than a matter of chance. It is therefore imprudent to suggest that the results given here represent any actual thermal profile from the Ballachulish aureole, rather they are a consequence of a methodology which needs more work and a geothermometer which has not yet been convincingly corroborated.

5) Potential for future study

Any attempts to rigorously test Ti in quartz as a valid geothermometry tool require significantly more work than was possible in the scope of this study. Initial focus must relate to redesigning the methodology before any real conclusions may be drawn about the geothermometer itself. There are also possibilities to use other facets of the distribution of Ti in quartz to derive temperatures. These are discussed below.

Determining the main CL activator in quartz samples
It has been shown that Ti may be important for causing cathodoluminescence in some cases where the greyscale and Ti (ppm) have a strong correlation, but in other cases it is not the main luminous component. The main CL activator must be determined for quartz grains before brightly luminescing edges are selected for EPMA. This could be done either using EPMA set to detect all potential luminescing components (e.g. Ti, Al, Li, Na, K etc) or by using external colour filters on the CL detector in order to isolate specific wavelengths (Ti luminesces most in the blue part of the spectrum, around 415nm wavelength; [*Spear and Wark*, 2009]). This would allow multiple CL images in different colours to be produced, which would in turn elucidate what is responsible for CL, if knowledge of the luminescence wavelength of each potential activator is known.

Producing temperature-time histories from diffusion of Ti away from rutile
Where a grain of rutile is present within a closed quartz crystal (e.g. Figure 3.5b), the diffusion of Ti away from that grain (as shown by greyscale variations on CL images) can be a powerful tool to determine T-t pathways. Using geospeedometry and inverse theory in a technique modified from *Lasaga and Jianxin* [1995], temperature can be extracted from multiple greyscale profiles which are essentially a proxy for the extent of Ti diffusion away from rutile grains.

Determining peak temperature using diffusion profiles into rutile
The previous point related to diffusion of Ti away from rutile within quartz, but it may also be possible to determine temperatures by looking at diffusion of Ti through quartz to form rutile needles as suggested by *Cherniak et al.* [2007]. If rutile has formed in quartz by diffusion, then there should be areas of Ti-depleted quartz surrounding rutile needles. Using the same principle of a temperature-dependent diffusivity of Ti in quartz [*Cherniak et al.*, 2007] as TitaniQ was based on, the size of Ti-depleted haloes around rutile needles could theoretically give temperatures.

Ascertaining the importance of a fluid phase and Ti speciation
Whilst it has been stated that fluids have certainly been ejected from the Ballachulish intrusion and subsequently mobilised around the aureole [*Holness and Clemens*, 1999], the importance of these fluids in causing Ti zoning is not entirely clear. This must first be established, and following that the probable speciation of Ti within these fluids (if present) must be understood [*Wilson et al.*, in press]. Pressure, temperature and pH together can constrain the likely Ti species present in a fluid. The former two parameters are generally known from previous work in geothermobarometry, and the latter may be determined by detailed fluid inclusion analysis. Determinations of the Ti species present in these natural examples must also be accompanied by experimental studies where the Ti uptake into quartz is monitored at different pressure and temperature conditions, and with different Ti species in solution.

6) Conclusions

This study has shown that whilst the TitaniQ geothermometer of *Wark and Watson* [2006] may give sensible results of crystallisation temperatures, there are many issues which must be considered before these results can be taken seriously. Firstly, cathodoluminescence activators in the samples must be constrained as the CL images are essentially a cornerstone of the methodology. Secondly, the concerns of various workers about the lack of concern by TitaniQ for rigorous thermodynamic derivation, pressure effects and the effect of Ti speciation must be somehow satisfied. The latter tasks will not be straightforward and may require the geothermometers to be rewritten to include the omitted parameters. This will surely be a timely process and may end up becoming so complex that the simplicity of geothermometry by measuring Ti in quartz is overridden, making the technique unviable.

The temperature-dependent diffusivity of titanium within quartz makes good thermodynamic sense and appears to be well-constrained. However, it is only when this construct is extrapolated into a geothermometer promising simple temperature determinations from an ubiquitous mineral that the problems arise. It is the strong recommendation of the author that work attempting to derive temperatures from titanium in quartz is suspended until a much greater knowledge of the complicating factors is gained.

Acknowledgements
The author would like to express his gratitude to Dr Geoffrey Lloyd and Dr David Banks for the co-supervision of this project. Thanks are also given to Dr Eric Condliffe for assistance with analytical equipment, Dr Daniel Morgan for useful discussions regarding the geothermometer, and Dr Dan Cornford of Aston University for assistance with statistical analysis.

References
Adamson, N. (2010), Applicability of TitaniQ and LA-ICP-MS analysis to metamorphic quartzite samples from the Moine thrust zone, NW Scotland. Unpublished MGeol Thesis, University of Leeds.

Allègre, C. J., A. Provost, and C. Jaupart (1981), Oscillatory zoning: A pathological case of crystal growth, *Nature*, *294*(5838), 223-228.

Bailey, E. B., and H. B. Maufe (1960), *The Geology of Ben Nevis and Glencoe and the Surrounding Country: Explanation of Sheet 53*.

Blankenburg, H.-J., J. Götze, and H. Schulz (1994), Quarzrohstoffe, *Deutscher Verlag für Grundstoffindustrie*.

Buntebarth, G. (1991), Thermal models of cooling, in *Equilibrium and Kinetics in Contact Metamorphism: The Ballachulish Igneous Complex and Its Aureole*, edited by G. Voll, J. Töpel, D. R. M. Pattison, and F. Seifert, pp. 379-402, Springer Verlag, Heidelberg.

Buntebarth, G., and G. Voll (1991), Quartz grain coarsening by collective crystallization in contact quartzites, in *Equilibrium and Kinetics in Contact Metamorphism: The Ballachulish Igneous Complex and Its Aureole*, edited by G. Voll, J. Töpel, D. R. M. Pattison, and F. Seifert, pp. 251-265, Springer Verlag, Heidelberg.

Cherniak, D. J., B. E. Watson, and D. Wark (2007), Ti diffusion in quartz, *Chemical Geology*, *236*(1-2), 65-74.

Dennen, W. H., W. H. Blackburn, and A. Quesada (1970), Aluminum in quartz as a geothermometer, *Contributions to Mineralogy and Petrology*, *27*(4), 332–342.

Fraser, G. L., D. R. M. Pattison, and L. M. Heaman (2004), Age of the Ballachulish and Glencoe Igneous Complexes (Scottish Highlands), and paragenesis of zircon, monazite and baddeleyite in the Ballachulish Aureole, *Journal of the Geological Society*, *161*(3), 47-462.

Guillong, M., D. L. Meier, M. M. Allan, C. A. Heinrich, and B. W. D. Yardley (2007), SILLS: A Matlab-based programme for the reduction of laser ablation ICP-MS data of homogeneous materials and inclusions, in *Laser Ablation ICP-MS in the Earth Sciences: current practices and outstanding issues*. *Mineralogical Association of Canada Short Course Series*, edited by P. Sylvester, pp. 328-333.

Götze, J., M. Plötze, T. Graupner, D. K. Hallbauer, and C. J. Bray (2004), Trace element incorporation into quartz: A combined study by ICP-MS, electron spin resonance, cathodoluminescence, capillary ion analysis, and gas chromatography, *Geochimica et Cosmochimica Acta*, *68*(18), 3741-3759.

Götze, J., M. Plötze, M. Tichomirowa, H. Fuchs, and J. Pilot (2001), Aluminium in quartz as an indicator of the temperature of formation of agate, *Mineralogical Magazine*, *65*(3), 407-413.

Hayden, L., and B. E. Watson (2007), Rutile saturation in hydrous siliceous melts and its bearing on Ti-thermometry of quartz and zircon, *Earth and Planetary Science Letters*, *258*(3-4), 561-568.

Hoernes, S., and G. Voll (1991), Detrital quartz and K-feldspar in quartzites as indicators of oxygen isotope exchange kinetics, in *Equilibrium and Kinetics in Contact Metamorphism: The Ballachulish Igneous Complex and Its Aureole*, edited by G. Voll, J. Töpel, D. R. M. Pattison, and F. Seifert, pp. 315-326, Springer Verlag, Heidelberg.

Holness, M. B., and J. D. Clemens (1999), Partial melting of the Appin Quartzite driven by fracture-controlled H2O infiltration in the aureole of the Ballachulish Igneous Complex, Scottish Highlands, *Contributions to Mineralogy and Petrology*, *136*(1-2), 154-168.

Holness, M., and G. Watt (2001), Quartz recrystallization and fluid flow during contact metamorphism: a cathodoluminescence study, *Geofluids*, *1*(3), 215–228.

Kawasaki, T., and Y. Osanai (2008), Empirical thermometer of TiO_2 in quartz for ultrahigh-temperature granulites of East Antarctica, *Geological Society, London, Special Publications*, *308*(1), 419-430.

Kohn, M. J., and C. J. Northrup (2009), Taking mylonites' temperatures, *Geology*, *37*(1), 47-50.

Kroll, H., C. Krause, and G. Voll (1991), Disordering, re-ordering and unmixing in alkali feldspars from contact-metamorphosed quartzites, in *Equilibrium and Kinetics in Contact Metamorphism: The Ballachulish Igneous Complex and Its Aureole*, edited by G. Voll, J. Töpel, D. R. M. Pattison, and F. Seifert, pp. 267-296, Springer Verlag, Heidelberg.

Kruhl, J. H., and M. Nega (1996), The fractal shape of sutured quartz grain boundaries: application as a geothermometer, *Geologische Rundschau*, *85*(1), 38.

Landtwing, M. R. (2005), Relationships between SEM-cathodoluminescence response and trace-element composition of hydrothermal vein quartz, *American Mineralogist*, *90*(1), 122-131.

Lasaga, A. C., and J. Jianxin (1995), Thermal History of Rocks: P-T-t Paths from Geospeedometry, Petrologic Data and Inverse Theory Techniques, *American Journal of Science*, *295*(6), 697–741.

Lind, A. (1996), *Microstructural Stability and the Kinetics of Textural Evolution*, Unpublished PhD Thesis, University of Leeds.

Mamtani, M. a, and R. O. Greiling (2010), Serrated quartz grain boundaries, temperature and strain rate: testing fractal techniques in a syntectonic granite, *Geological Society, London, Special Publications*, *332*(1), 35-48.

Masch, L., and S. Heuss-Assbichler (1991), Decarbonation reactions in siliceous dolomites and impure limestones, in *Equilibrium and Kinetics in Contact Metamorphism: The Ballachulish Igneous Complex and Its Aureole*, edited by G. Voll, J. Töpel, D. R. M. Pattison, and F. Seifert, pp. 211-227, Springer Verlag, Heidelberg.

Müller, A., R. Herrington, R. Armstrong, R. Seltmann, D. J. Kirwin, N. G. Stenina, and A. Kronz (2010), Trace elements and cathodoluminescence of quartz in stockwork veins of Mongolian porphyry-style deposits, *Mineralium Deposita*, *45*(7), 707-727.

Müller, A., M. Wiedenbeck, A. M. van den Kerkhof, A. Kronz, and K. Simon (2003), Trace elements in quartz – a combined electron microprobe, secondary ion mass spectrometry, laser-ablation ICP-MS, and cathodoluminescence study, *European Journal of Mineralogy*, *15*(4), 747-763.

Pattison, D. (1991), P-T-a(H2O) conditions in the thermal aureole, in *Equilibrium and Kinetics in Contact Metamorphism: The Ballachulish Igneous Complex and Its Aureole*, edited by G. Voll, J. Töpel, D. R. M. Pattison, and F. Seifert, pp. 327-350, Springer Verlag, Heidelberg.

Pattison, D. R. M. (1989), P-T Conditions and the Influence of Graphite on Pelitic Phase Relations in the Ballachulish Aureole , Scotland, *Journal of Petrology*, *30*(1985), 1219-1244.

Pattison, D. R. M., and B. Harte (1997), The geology and evolution of the Ballachulish Igneous Complex and Aureole, *Scottish Journal of Geology*, *33*(1), 1-29.

Pattison, D. R. M., and G. Voll (1991), Regional geology of the Ballachulish area, in *Equilibrium and Kinetics in Contact Metamorphism: The Ballachulish Igneous Complex and Its Aureole*, edited by G. Voll, J. Töpel, D. R. M. Pattison, and F. Seifert, pp. 19-38, Springer Verlag, Heidelberg.

Pearce, N. J. G., W. T. Perkins, J. a Westgate, M. P. Gorton, S. E. Jackson, C. R. Neal, and S. P. Chenery (1997), A Compilation of New and Published Major and Trace Element Data for NIST SRM 610 and NIST SRM 612 Glass Reference Materials, *Geostandards and Geoanalytical Research*, *21*(1), 115-144.

Perny, B., P. Eberhardt, K. Ramseyer, J. Mullis, and R. Pankrath (1992), Microdistribution of Al, Li, and Na in α quartz: possible causes and correlation with short-lived cathodoluminescence, *American Mineralogist*, *77*(5-6), 534-544.

Reed, S. J. B. (1996), *Electron Microprobe Analysis and Scanning Electron Microscopy in Geology*, Cambridge University Press, Cambridge.

Rusk, B. G., H. a Lowers, and M. H. Reed (2008), Trace elements in hydrothermal quartz: Relationships to cathodoluminescent textures and insights into vein formation, *Geology*, *36*(7), 547.

Rusk, B. G., M. H. Reed, J. H. Dilles, and A. J. R. Kent (2006), Intensity of quartz cathodoluminescence and trace-element content

in quartz from the porphyry copper deposit at Butte, Montana, *American Mineralogist*, *91*(8-9), 1300-1312.

Sato, K., and M. Santosh (2007), Titanium in quartz as a record of ultrahigh-temperature metamorphism: the granulites of Karur, southern India, *Mineralogical Magazine*, *71*(2), 143-154.

Sawakuchi, A. O., R. DeWitt, and F. M. Faleiros (2011), Correlation between thermoluminescence sensitivity and crystallization temperatures of quartz: Potential application in geothermometry, *Radiation Measurements*, *46*(1), 51-58.

Spear, F. S., and D. Wark (2009), Cathodoluminescence imaging and titanium thermometry in metamorphic quartz, *Journal of Metamorphic Geology*, *27*(3), 187-205.

Storm, L. C., and F. S. Spear (2009), Application of the titanium-in-quartz thermometer to pelitic migmatites from the Adirondack Highlands, New York, *Journal of Metamorphic Geology*, *27*(7), 479-494.

Thigpen, J. R., R. D. Law, G. E. Lloyd, S. J. Brown, and B. Cook (2010), Deformation temperatures, vorticity of flow and strain symmetry in the Loch Eriboll mylonites, NW Scotland: Implications for the kinematic and structural evolution of the northernmost Moine Thrust zone, *Geological Society Special Publication*, (335), 623-662.

Thomas, J. B., B. E. Watson, F. S. Spear, P. T. Shemella, S. K. Nayak, and A. Lanzirotti (2010), TitaniQ under pressure: the effect of pressure and temperature on the solubility of Ti in quartz, *Contributions to Mineralogy and Petrology*, *160*(5) 743-759

Vazquez, J. a, S. F. Kyriazis, M. R. Reid, R. C. Sehler, and F. C. Ramos (2009), Thermochemical evolution of young rhyolites at Yellowstone: Evidence for a cooling but periodically replenished postcaldera magma reservoir, *Journal of Volcanology and Geothermal Research*, *188*(1-3), 186-196.

Voll, G. (1991), The setting of the Ballachulish intrusive igneous complex in the Scottish Highlands, in *Equilibrium and Kinetics in Contact Metamorphism: The Ballachulish Igneous Complex and Its Aureole*, edited by G. Voll, J. Töpel, D. R. M. Pattison, and F. Seifert, pp. 3-17, Springer Verlag, Heidelberg.

Wark, D., W. Hildreth, F. S. Spear, D. J. Cherniak, and B. E. Watson (2007), Pre-eruption recharge of the Bishop magma system, *Geology*, *35*(3), 235-238.

Wark, D., and B. E. Watson (2006), TitaniQ: a titanium-in-quartz geothermometer, *Contributions to Mineralogy and Petrology*, *152*(6), 743-754.

Watt, G. (1997), Cathodoluminescence and trace element zoning in quartz phenocrysts and xenocrysts, *Geochimica et Cosmochimica Acta*, *61*(20), 4337-4348.

Weiss, S., and G. Troll (1989), The Ballachulish Igneous Complex, scotland: Petrography, mineral chemistry, and order of crystallization in the monzodiorite-quartz diorite suite and in the granite, *Journal of Petrology*, *30*(5), 1069-1115.

Weiss, S., and G. Troll (1991), Thermal conditions and crystallisation sequences as deduced from whole-rock and mineral chemistry, in *Equilibrium and Kinetics in Contact Metamorphism: The Ballachulish Igneous Complex and Its Aureole*, edited by G. Voll, J. Töpel, D. R. M. Pattison, and F. Seifert, pp. 67-98, Springer Verlag, Heidelberg.

Wiebe, R. a, D. Wark, and D. P. Hawkins (2007), Insights from quartz cathodoluminescence zoning into crystallization of the Vinalhaven granite, coastal Maine, *Contributions to Mineralogy and Petrology*, *154*(4), 439-453.

Wilson, C., T. Seward, B. Charlier, A. Allan, L. Bello, and W. Hildreth (in press), An assessment of the validity of temperature and pressure estimates from Ti concentrations in magmatic and hydrothermal quartz, *Contributions to Mineralogy and Petrology*.

Wu, X.-Q., D.-L. Liu, Z.-S. Li, and Q. Yang (2006), A new fractal method for the determination of deformation temperatures and strain rates - A case study of the Fuchashan tectonite in the Tanlu fault, *Geology in China*, *33*(1), 153-159.

56148		56158		56183		56169	
Spot Number	ppm Ti	Spot Number	ppm Ti	Spot Number	ppm Ti	Spot Number	ppm Ti
56148_001	60	56158_001	10	56183_001	30	56169_001	0
56148_002	80	56158_002	10	56183_002	20	56169_002	20
56148_003	40	56158_003	40	56183_003	10	56169_003	20
56148_004	30	56158_016	1470	56183_004	0	56169_004	40
56148_005	40	56158_017	10	56183_005	0	56169_005	0
56148_006	60	56158_018	0	56183_006	40	56169_006	30
56148_007	50	56158_019	50	56183_007	10	56169_007	20
56148_008	40	56158_020	0	56183_008	10	56169_008	30
56148_009	50	56158_021	10	56183_009	20	56169_009	20
56148_010	60	56158_022	10	56183_010	20	56169_010	50
56148_011	20	56158_023	0	56183_011	0	56169_011	20
56148_012	60	56158_024	30	56183_012	20	56169_012	10
56148_013	80	56158_025	100	56183_013	30	56169_013	30
56148_014	90	56158_026	10	56183_014	30	56169_014	0
56148_015	40	56158_027	20	56183_015	0	56169_015	30
56148_016	70	56158_051	20	56183_016	10	56169_016	30
56148_017	50	56158_052	80	56183_017	20	56169_017	10
56148_018	80	56158_053	0	56183_018	30	56169_018	130
56148_019	50	56158_054	10	56183_019	30	56169_019	20
56148_020	40	56158_055	10	56183_020	10	56169_020	10
56148_021	50	56158_056	30	56183_021	0	56169_021	30
56148_022	60	56158_057	10	56183_022	40	56169_022	10
56148_023	50	56158_058	30	56183_023	10	56169_023	30
56148_024	20	56158_059	30	56183_024	50	56169_024	40
56148_025	0	56158_060	10	56183_025	110	56169_025	20
56148_026	60			56183_026	20	56169_026	10
56148_027	90			56183_027	10	56169_027	100
56148_028	0			56183_028	20	56169_028	0
56148_029	70			56183_029	70	56169_029	30
56148_030	630			56183_030	50	56169_030	20
56148_046	30			56183_031	10	56169_031	10
56148_047	40			56183_032	30	56169_032	10
56148_048	80			56183_033	30	56169_033	0
56148_049	80			56183_034	10	56169_034	0
56148_050	50			56183_035	40	56169_035	10
56148_051	70			56183_037	30	56169_036	10
56148_052	30			56183_038	0	56169_037	10
56148_053	60			56183_039	30	56169_038	10
56148_060	80			56183_040	20	56169_039	50
				56183_041	40	56169_040	0
						56169_041	0
						56169_042	30
						56169_043	30
						56169_044	0
						56169_045	30
						56169_046	20
						56169_047	20
						56169_048	0
						56169_049	40
						56169_050	80
						56169_051	0
						56169_052	10
						56169_053	50
						56169_054	50
						56169_055	40
						56169_056	60
						56169_057	30
						56169_058	80
						56169_059	20
						56169_060	40
Average	**53**		**22**		**24**		**26**

Appendix 1: All Ti spot analyses with ppm Ti as determined by Jeol ZAF software. Where numbers are missing, line analyses rather than points were taken (a total of 60 measurements were taken from each sample, such that 56158 would have the most line analysis and 56169 the least). Grey highlighting is where rutile was accidentally sampled. These are omitted from the mean.